59TH ANNUAL CONFERENCE ON

MAGNETISM AND MAGNETIC MATERIALS

3-7 NOVEMBER 2014 • HONOLULU, HAWAII

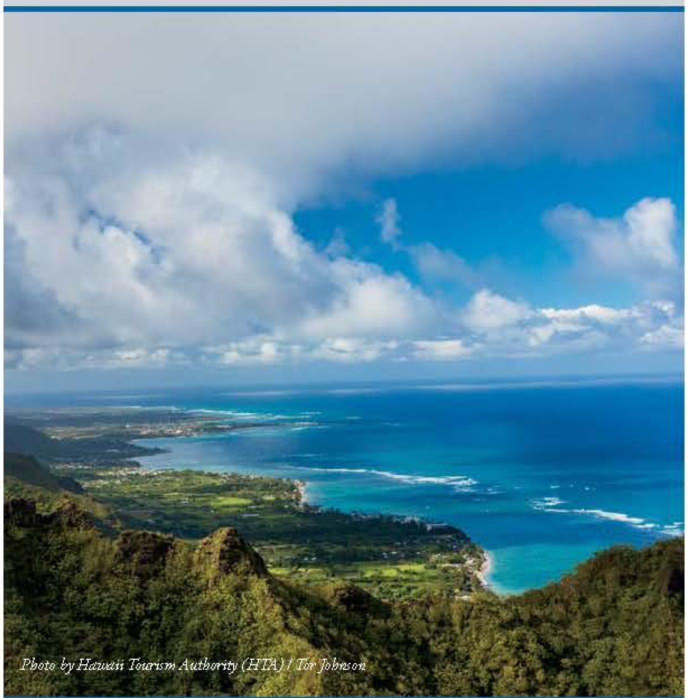

Photo by Hawaii Tourism Authority (HTA) / Tor Johnson

PROGRAM

MMM 2014 Honolulu

AIP Publishing

IEEE MAGNETICS 50 YEARS 1964 2014

Jointly sponsored by AIP Publishing, LLC and the IEEE Magnetics Society

AP-08. Influence of Sleeve Material on Mechanical Stress of Permanent Magnet in High-speed Rotor. *J. Ahn*[2,1], K. Kim[1], H. Park[1], C. Park[2] and S. Jang[1] *1. Electrical Engineering, Chungnam National university, Daejun, Republic of Korea; 2. Advanced Manufacturing Systems Research Division, Korea Institute of Machinery and Materials, Daejeon, Republic of Korea*

AP-09. RF power absorption effects of FeCo hollow fibers composite and sendust flakes composite. *B. Nam*[1], J. Lee[1], J. Kim[1] and K. Kim[1] *1. Physics, Yeungnam University, Gyeongsan, Republic of Korea*

AP-10. Design of broadband circulator based on Gyromagnetic materials and substrate integrated waveguide. C. Huang[1,2] and *H. Lu*[1,2] *1. National Engineering Research Center of Electromagnetic Radiation Control,UESTC, Chengdu, Sichuan, China; 2. State Key Laboratory of Electronic Thin Films and Integrated Devices,UESTC, Chengdu, Sichuan, China*

AP-11. Thermal conductivity prediction of magnetic composite sheet for near-field electromagnetic absorption. *J. Lee*[1], J. Kim[1], B. Nam[1] and K. Kim[1] *1. Physics, Yeungnam University, Gyeongsan, Republic of Korea*

AP-12. Electroacoustic Excitation and Detection of Magnetic Oscillations in ZnO-YIG-GGG Magnetoelectric Bulk Acoustic Wave Resonator. *N. Polzikova*[1], S. Alekseev[1,2], I. Kotelyanskii[1], V. Luzanov[1] and A. Raevskiy[1,2] *1. Kotel'nikov Institute of Radio-engineering and Electronics of RAS, Moscow, Russian Federation; 2. Moscow Institute of Physics and Technology, Dolgoprudny, Moscow reg., Russian Federation*

AP-13. Effect of Magnetization Pattern on Partial Demagnetization of Permanent Magnet Machine with Ferrite Magnet. *K. Kim*[1], J. Ahn[1], J. Choi[1] and S. Jang[1] *1. Chungnam National Univercity, Daejeon, Republic of Korea*

AP-14. Design and Characteristics Analysis of Linear Oscillatory Actuator Using Ferrite Permanent Magnet for Refrigerator Compressor. *K. Kim*[1], H. Park[1], J. Choi[1] and S. Jang[1] *1. Chungnam National University, Daejeon, Republic of Korea*

AP-15. Copper (Cu) Substituted NiZn Ferrite for 125 kHz Wireless Power Transfer (WPT) Application. *I. Baek*[1], N. Kim[1], N. Hur[1], W. Seong[1], W. Lee[2], Y. Hong[2], H. Kim[3] and J. Kim[3] *1. Research and Development Center, EMW Company, Seoul, Republic of Korea; 2. Department of Electrical and Computer Engineering and MINT Center, The University of Alabama, Tuscaloosa, AL; 3. Department of Electrical Engineering, Korea Advanced Institute of Technology, Daejeon, Republic of Korea*

AP-16. Experimental Characterization of Slinky Laminated Core and Iron Loss Analysis of Electrical Machine. *M. Lim*[1], S. Hwang[1], K. Jung[1], J. Kim[1] and J. Hong[1] *1. Automotive Engineering, Hanyang University, Seoul, Republic of Korea*

Experimental Characterization of Slinky Laminated Core and Iron Loss Analysis of Electrical Machine

M.S. Lim[1], J.H. Kim[2], and J.P. Hong[1*]

[1]Department of Automotive Engineering, Hanyang University, Seoul 133-791, Korea

[2]POSCO Global R&D Center, Incheon 406-840, Korea

*Corresponding Author

Abstract

The magnetic properties of a motor core are deteriorated by slinky lamination method due to the mechanical stress and strain in core materials. To analyze the iron loss of an electrical machine with a slinky-laminated stator, material experiments using the stator core were conducted. With the examined material data, the iron loss of the proposed motor was investigated using the finite-element method (FEM). To verify the validity of the material experiment and FEM, the proposed motor was subjected to a no-load test and a mechanical loss test. Based on the test results and through the loss decomposition process, the actual iron loss of the motor was obtained and was compared with the FEM results.

1. Introduction

With the development of the manufacturing technique and production machines, the slinky lamination method is now being used to significantly reduce the material waste [1]. For this process, a long iron band is rolled up in a spiral way and is bonded. Thus, compressive stress in the inner part of the neutral axis and tensile stress in the outer part of the axis, and strain occur simultaneously in the core. As a result, the magnetic properties are deteriorated.

There have been several studies on the influence of shrink fitting [2], [3]. Only the impact of the compressive stress was examined, however, and this was done. This cannot be considered suitable for accurately analyzing the iron loss of the slinky-laminated core in electrical machines.

In this work, an outer-rotor surface-mounted permanent-magnet synchronous motor (SPMSM) for a washing machine with a slinky-laminated stator is proposed as organized in Table I. A material test using the slinky-laminated stator of the motor was conducted to obtain the deteriorated *B-H* curve and iron loss data for several levels of excitation field at several frequencies. In addition, the total iron loss of the motor was obtained by the finite-element method (FEM) using the deteriorated material data. Finally, the validity of the material test and of the FEM was verified through the experiment that was performed on the proposed SPMSM.

2. Magnetic Properties of Slinky Laminated Core and Stacked Core

2.1 Experiment for deteriorated Material Properties

To measure the *B-H* curve and iron loss under stresses and strain condition, a slinky ring core from a stator yoke was prepared using a wire cut as shown in Fig. 1, and the dimensions of the test yoke are shown in Table II. Insulation tape was then wound around the ring core for insulation purposes. For primary coil N_1 and secondary coil N_2, 200 and 40 turns were used to guarantee the exciting of a high field (over 5kA/m). The *B*-*H* curve and iron loss test were conducted as per IEC 60404-6. The *H* field is measured at the primary coil, and the *B* field is measured at the secondary coil. The *B*-*H* hysteresis loop was measured to measure the iron loss.

2.2 Iron Loss Separation

To interpolate and extrapolate the loss properties of the material, the phenomenological principle was adopted [4]. According to the principle, the average power loss density of a machine W_{Core} can be decomposed into three components as equation (1):

$$W_{Core} = W_{Hysteresis} + W_{Eddy} + W_{Anomalous} \quad [W/kg] \ (1)$$

where $W_{Hysteresis}$ is the quasi-static hysteresis loss, W_{Eddy} is the macroscopic eddy current loss, and $W_{Anomalous}$ is the excess loss (dynamic behavior of the magnetic domains), as shown in equations (2)-(4) [4]. Analytical models have been proposed to investigate these components, which require the identification of the parameters. Thus, for a sinusoidal supply, the static losses can be approximated by the following equation proposed by Steinmetz, where B is the peak value of the magnetic flux density, f is the frequency, and α and β are the Steinmetz coefficients.

$$W_{Hysteresis} = k_h f B^{\alpha} \quad [W/kg] \ (2)$$

$$W_{Eddy} = k_e f^2 B^2 \quad [W/kg] \ (3)$$

$$W_{Anomalous} = k_a f^{1.5} B^{\beta} \quad [W/kg] \ (4)$$

To identify the coefficients, the iron losses should be examined for several magnetic flux densities and frequencies, and the least-square method (LSM) was used for this purpose. Based on the comparison of the magnetic properties of the stacked and slinky-laminated cores as shown in Fig. 2, it is confirmed that iron loss of the slinky-laminated core was 18.14% larger than the normally stacked core at 50 Hz.

3. Loss Analysis of Proposed Motor

3.1 Finite Element Analysis

With the normal material data and the deteriorated material data examined above, the total iron loss of the motor was analyzed via FEM. Fig. 3 shows the process of determining the total iron losses, which is described in 5 steps [5]. Step 1: Using nonlinear FEA, the flux density at each mesh for one electrical angle period is calculated, as the rotor is rotated. Here, the flux density is calculated as the normal and tangential components. Step 2: Using the flux density from step 1, Fourier transform is performed to find the magnitude of the fundamental and harmonic components. Step 3: From the iron loss data for the material, the iron loss corresponding to the frequency and flux density of each harmonic is calculated. The material information is based on the empirical data. Step 4: The sum of the iron loss due to the harmonic components at each mesh is calculated. Step 5: The iron losses of all the meshes are added to determine the total iron loss of the machine.

3.2 Experiments and verification

In this study, two kinds of experiments as shown in Fig. 4 and the loss decomposition process were conducted to find the total iron loss of the proposed motor. First, using the drive motor, the test-motor-assembled stator and rotor was controlled to evaluate the total loss of the test motor under the no-load condition. This loss consisted of iron loss, mechanical loss, and copper loss. T_{SR} and ω_{SR} are the torque and rotation speed under the steady-state condition. The subscript *SR* refers to the test-motor-assembled stator and rotor. The second test was conducted with only the rotor of the test motor was installed in the experiment set to measure the mechanical loss, and the torque and rotational speed under this condition was subscripted as *R*. T_R and ω_R are the torque and rotation speed under the steady-state condition.

Through the experiments described above, the total iron loss of the motor according to the speed was calculated using equation (5). The copper loss is negligible because the input current is extremely small. Given the calculation result shown in Fig. 5, the iron loss can be said to account for around 82% of the total no-load loss.

$$W_{Iron} = W_{Total\ no-load\ Loss} - W_{Mechanical\ Loss} = T_{SR} \cdot \omega_{SR} - T_R \cdot \omega_R \quad [W] \ (5)$$

Finally, Fig. 6 shows the experiment and FEM results considering the slinky-laminated material data. The validity of the material test method and loss analysis process shown in the paper was verified through the comparison of the FEM and experiment results. The cause of the error is the use of the same material data at the teeth and yoke for FEM. Teeth, however, are rarely stressed by the slinky lamination method. Also, the error occurs in the interpolation and extrapolation of the material data using the Steinmetz equations. Nevertheless, the iron loss of the simulation is similar to that of the experiment.

4. Conclusion

In this paper, the influence of the slinky lamination method as a manufacturing process on the iron loss was investigated. With the deteriorated material data examined, the iron loss of the proposed motor was analyzed via FEM. The motor was subjected to a no-load test and a mechanical loss test, and it was compared with the FEM result to verify the validity of the material data, loss analysis, and loss decomposition process presented in this paper.

Acknowledgments

This research was supported by the MKE (The ministry of Knowledge Economy), Korea, under the CITRC (Convergence Information Technology Research Center) support program (NIPA-2013-H0401-13-1008) supervised by the NIPA (National IT Industry Promotion Agency).

References

[1] F. Libert, *et al.*, *IET Proceedings of the IET Power Electronics, Machines and Drives (PEMD)*, Dublin, Ireland, 4-6 April 2006, pp. 676-680

[2] D. Miyagi, *et al*., *IEEE Trans. Magn.*, Vol. 46, No. 2, pp. 318-321(2010)

[3] N. Takahashi, *et al*., *IEEE Trans. Magn.*, Vol. 43, No. 6, pp. 2749-2751(2007)

[4] R. Ramarotafika, *et al*., *IEEE Trans. Magn.*, Vol. 48, No. 4, pp. 1629-1632(2012)

[5] B. H. Lee, *et al*., *IEEE Trans. Magn.*, Vol. 47, No. 5, pp. 1066-1069(2011)

List of Table

TABLE I
SPECIFICATIONS OF THE PROPOSED MOTOR

Quantity	Unit	Value
Maximum voltage	V_{DC}	310
Maximum current	A_{peak}	10
Torque (washing / dehydrating mode)	Nm	37 / 2
Speed (washing / dehydrating mode)	rpm	46 / 1200
Rotor / stator diameter	mm	283 / 265
Stack length of the stator	mm	24
Overhang (magnet / stator)	%	136.67
Pole / slot number	-	48 / 36
Magnet material	-	Ferrite
Stator core material	-	Cold rolled steel sheet (1mm)

TABLE II
MATERIAL TEST CONDITION

Winding (turns)		Dimensions (mm)		Properties	
Primary	Secondary	Outer / Inner diameter	Height	Mass (g)	Density (g/dm³)
200	40	200.3 / 194.6	13.4	230.68	7.85

List of Figures